Sinusoidal Bragg grating based on hybrid metal insulator metal plasmonic waveguide

Sindhura Chitimireddy ✉, *Prateeksha Sharma, Dinesh Kumar Vishwakarma*

Discipline of Electronics and Communication Engineering, PDPM Indian Institute of Information Technology, Design and Manufacturing, Jabalpur, MP 482005, India
✉ *E-mail: sindhurareddy234@gmail.com*

Published in Micro & Nano Letters; Received on 28th April 2018; Revised on 15th July 2018; Accepted on 24th July 2018

This is the first report on 3D sinusoidal Bragg grating structure based on hybrid metal insulator metal (HMIM) plasmonic waveguide. The proposed structure has a gradual change in the refractive index rather than an abrupt change providing excellent filtering characteristics. The device is studied at an operating wavelength of 1.55 μm. The results are based on numerical simulations performed using the software CST microwave studio suite. The transmission characteristics show more than 80% transmission in the passband and near zero transmission in the rejection band. The proposed structure reduces the scattering losses and a wide bandgap of 0.387 μm is achieved. The proposed structure has a track length of 3.784 μm for 11 cells, which is very less compared to previous reports allowing large-scale integration of photonic devices. A microcavity is also formed and its resonance is investigated by introducing a defect length of 0.217 μm in the periodic structure. A peak transmission of 50% and a narrow resonance bandwidth of 0.029 μm are achieved at 1.55 μm resonance wavelength. The quality factor which defines the energy stored in the cavity is $Q = 53$.

1. Introduction: The availability of nanofabrication techniques and high-performance computational resources opened up the applications of plasmonic devices in integrated photonics, all optical chips, solar cells, biosensors and so on. Though the plasmonic waveguides possess strong light confinement, the major limitation is that they suffer from large propagation losses [1]. Furthermore, two main kinds of the plasmonic waveguides are proposed: metal–insulator–metal (MIM) and insulator–metal–insulator (IMI). These waveguides suffer from the trade-off between propagation length and field confinement. The dielectric waveguides, in contrast, provide low losses but suffer from diffraction limit and are larger in size. Merging the guiding mechanisms of plasmonic and dielectric waveguides, various kinds of hybrid plasmonic waveguides are proposed, which provides a solution to the limitations faced by the conventional dielectric and standard plasmonic waveguides [2–4]. Few articles based on hybrid metal–insulator (HMI) plasmonic waveguides have been reported [5, 6]. However, they are mostly 1D structures which are practically not implementable. A study on plasmonic waveguide based on hybrid IMI (HIMI) has been reported providing long range propagation and sub-wavelength confinement [7]. To further enhance the light confinement and to lessen the propagation losses, a multi-layered hybrid MIM (HMIM) plasmonic waveguide has been reported [8]. The components like bends, couplers, power dividers, ring resonators and logic gates have been reported earlier based on HMIM plasmonic waveguides [8–10]. However, there are only a few reports on Bragg reflectors and filters based on HMIM plasmonic waveguide [11], but more are needed to be explored.

In the literature, there are some reports on MIM plasmonic waveguides and graphene based Bragg reflectors, but they offer poor performance [12–15] and the explanation is as follows. The MIM based 2D Bragg grating structures have been reported in [12–14], which are not realistic as thickness is not finite. Besides MIM waveguides are prone to excessive ohmic loss and HMIM waveguides are superior in this aspect [8–10]. The structure proposed in [16] is a MIM sinusoidal Bragg grating, which gives better performance than rectangular ones proposed in [12–15], yet this is again a 2D structure. A Bragg structure based on HMI plasmonic waveguide with grating incorporated by periodically varying the thicknesses of dielectric layers has also been reported in [17]. Different from that a rectangular Bragg grating in an HMIM plasmonic waveguide has been reported recently which incorporates a periodic variation of waveguide width [11]. Though this is a realistic 3D structure, it suffers poor transmission in passband due to abrupt changes in waveguide width, resulting in significant radiation losses. These losses could be mitigated by gradual width modulation of the hybrid plasmonic waveguide for realisation of grating. With this motivation, we propose and analyse a sinusoidal Bragg grating in a realistic HMIM plasmonic waveguide, which to the best of our knowledge is the first report of its kind.

The proposed structure is simulated using frequency domain solver of CST microwave (MW) studio suite, an electromagnetic computational tool which uses finite element method, a numerical method to solve electromagnetic equations. The perfectly matched layer (PML) absorbing boundary condition with a mesh density of 15 tetrahedrons per wavelengths is adopted and S-delta convergence test is performed to ensure accurate results.

The proposed structure shows high transmission in the passband while nearly zero transmission within the bandgap, thus having superior performance compared to the rectangular structure. Track length of the proposed sinusoidal Bragg gating is 3.784 μm for 11 cells, which is very small compared to the previous literature [16, 17]. Further, a microcavity is also formed and investigated for the resonant mode within the bandgap. The proposed sinusoidal Bragg gating is a realistic structure, compatible with the semiconductor fabrication process and hence useful for future chip scale applications. Different layers of the waveguide can be deposited by some standard techniques like silver layer by metallisation, silicon and silica layers by magnetron sputtering or plasma enhanced chemical vapour deposition process. Then e-beam lithography or focused ion beam can be used for patterning of the structure [2, 18–20].

2. Principle and design: The cross-sectional view of HMIM plasmonic waveguide is shown in Fig. 1*a*, where '*Z*' is the direction of propagation. Silver is chosen for the metal layer in the HMIM waveguide. The permittivity of metal is expressed by Drude model as [7]

$$\varepsilon = \varepsilon_{\infty} - \frac{\omega_p^2}{\omega^2 + j\omega\Gamma} \tag{1}$$

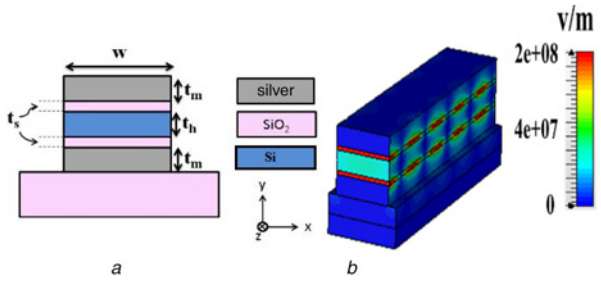

Fig. 1 *HMIM plasmonic waveguide*
a Cross-sectional view
b 3D *E*-field view

Here the dielectric constant at an infinite angular frequency ε_∞, bulk plasma frequency ω_p and collision frequency Γ are set as follows: $\varepsilon_\infty = 1$, $\omega_p = 1.39 \times 10^{16}$ rad/s, $\Gamma = 3.08 \times 10^{13}$/s at 1.55 μm wavelength. Thus the permittivity of silver at 1.55 μm is $-129 + 3.3i$ [21]. The refractive indices of silicon and silica are 3.48 and 1.44, respectively. The thicknesses of the high dielectric layer and the metallic layer are set to be $t_m = t_h = 0.10$ μm and thickness of low dielectric (spacer) layer is set as $t_s = 0.02$ μm. The operating wavelength range is 1–2 μm. In HMIM plasmonic waveguide, the coupling of both plasmonic mode (at Ag–SiO_2 interface) and conventional dielectric mode (at Si–SiO_2 interface) takes place providing a hybrid plasmonic mode. The role of silicon here is to provide a dielectric mode in plasmonic structure. Hence the propagation of light takes place through the two narrow spacer layers, as shown in Fig. 1*b*. The silica substrate is preferred since it offers low cost with high integration density.

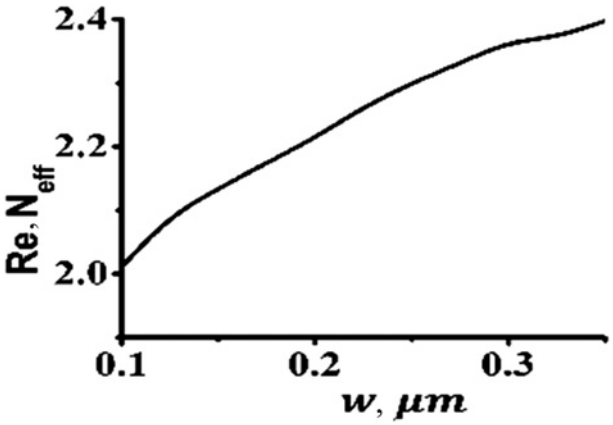

Fig. 2 *Re{N_{eff}} variation with respect to waveguide width at 1.55 μm operating wavelength*

Real part of the effective refractive index ($\mathrm{Re}\{N_{\mathrm{eff}}\} = \beta/k_0$, where β is the phase constant and k_0 is the wave number) variation with respect to waveguide width (w) is numerically evaluated and is shown in Fig. 2. It shows that waveguide dispersion properties are highly dependent on width variation. The $\mathrm{Re}\{N_{\mathrm{eff}}\}$ increases with increase in waveguide width reason being increased thickness of high index medium. As the silicon core gets broader, more EM field will stay in the high index core, which results in increased real part of N_{eff} [22]. This phenomenon is further used for designing Bragg grating.

Bragg grating is generally formed by the periodic variation of real part of the effective refractive index and it can be varied by various methods such as by varying material or geometrical parameters or using some non-linear phenomena. Here, we have adopted waveguide width variations for changing $\mathrm{Re}\{N_{\mathrm{eff}}\}$ periodically, as it depends on waveguide width almost linearly, which is shown in Fig. 2. We consider two different widths, $w_1 = 0.30$ μm and $w_2 = 0.15$ μm for efficient dominant mode propagation. The $\mathrm{Re}\{N_{\mathrm{eff}}\}$ for widths 0.30 and 0.15 μm are 2.366 and 2.134, respectively, at the operating wavelength of 1.55 μm as obtained in Fig. 2. The construction dimensions of a unit cell of rectangular Bragg grating with two subsections of lengths l_1 and l_2 are shown in Fig. 3*a*. The structure has been designed so that the following Bragg condition is met [11]:

$$\mathrm{Re}\{N_{\mathrm{eff}\,1}\} * l_1 + \mathrm{Re}\{N_{\mathrm{eff}\,2}\} * l_2 = \frac{\lambda_{\mathrm{B}}}{2} \tag{2}$$

Here λ_{B} is the Bragg wavelength. The lengths of two subsections of the unit cell are calculated using the above mentioned equation. Light gets reflected from the interfaces created due to the change in the width of the waveguide. It gives rise to constructive interference, resulting in strong reflection at the central wavelength λ_{B} in a certain range forming a bandgap. However, the rectangular Bragg grating shown in Fig. 3*a* does not offer decent transmission in the passband, as discussed earlier. Hence, here we propose sinusoidal Bragg grating for gradual changes in width, as shown in Fig. 3*b*. The sinusoidal Bragg gratings designed with N number of cells are shown in Fig. 3*c*.

3. Results and discussion: In this Letter, Bragg grating in HMIM plasmonic waveguide is formed by modulating the width of the waveguide according to sine-wave profile, where there is gradual variation in the width of the waveguide as shown in Fig. 3*b*.

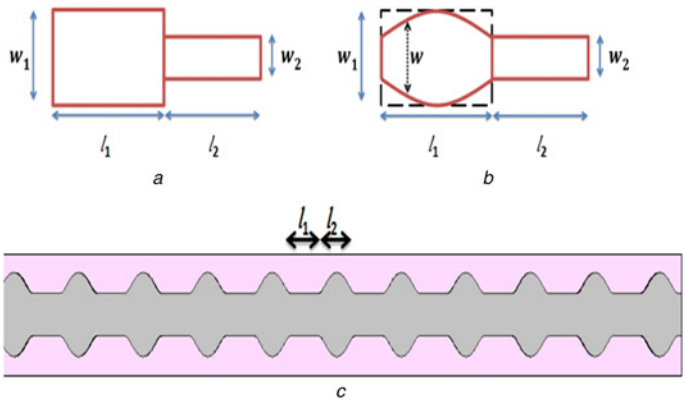

Fig. 3 *Construction dimensions of the unit cell for*
a Rectangular Bragg grating and
b Sinusoidal Bragg grating
c Top view of sinusoidal Bragg grating with N cells

doi: 10.1049/mnl.2018.5107

Therefore, it indirectly implies the gradual change in refractive index of the waveguide. This modification lessens the losses due to sharp bends, minimising the side lobe reflections that occur in the transmission band of rectangular Bragg grating. However, there will be a reduction in the bandgap of sinusoidal Bragg grating. The sinusoidal equation used to construct the grating structure is $\{ w = ((w_1 - w_2)/2)*(1 - \sin(\pi*t/l_1))\}$, where w, w_1 and w_2 represent respective widths as shown in Fig. 3*b* and 't' the length of unit cell subsection varies from 0 to l_1. The performance of the sinusoidal Bragg grating has been evaluated for various duty cycles to broaden the bandgap. The duty cycle is defined as $d = l_1/(l_1 + l_2)$. Lengths of respective subsections are calculated using (2) for respective duty cycle. The transmission characteristics of the sinusoidal Bragg grating with $N = 11$ cells for different duty cycles 0.2, 0.5 and 0.7 have been shown in Fig. 4. The number of Bragg cells is chosen so as to maximise the extinction ratio. It can be observed from Fig. 4 that the Bragg wavelength is insensitive to the duty cycle. A wide bandgap of 0.387 μm is achieved when 50% (i.e. $l_1 = l_2 = 1.172$ μm) duty cycle is considered. On changing the duty cycle, the bandgap reduces due to fewer reflections in the bandgap region. So, 50% duty cycle is fixed for further investigations.

The transmission and reflection characteristics of sine modulated Bragg grating are also observed by varying the number of unit cells ($N = 7$, 11 and 17), as shown in Fig. 5. On increasing the number of cells, there is a maximum reflection in the rejection band but at the same time transmission percentage is also reduced in the passband. Bragg grating gives a bandgap for any number of cells, but it does not offer near zero transmission in bandgap which is the required condition for ideal filtering characteristics. We achieve near zero transmission (<1%) in the bandgap for at least $N = 11$, whereas in the earlier reports, a minimum number of 17 cells were required to achieve near zero transmission in the bandgap. Track length of sinusoidal Bragg grating is 3.784 μm using 11 cells, which is much smaller compared to the previous reports. In [16] a track length of 11.22 μm for 17 cells, in [17] a track length of 6.46 μm for 18 cells and in [11] a track length of 4.063 μm for 11 cells have been reported.

The 3D *E*-field distributions have also been demonstrated for two wavelengths, i.e. 1.25 and 1.55 μm which occur in the pass band and bandgap regions, respectively. It is clearly distinguishable from Fig. 6 that there is light transmission in case of 1.25 μm whereas the light is completely reflected back in case of 1.55 μm.

To observe the abruptness behaviour, transmission characteristics are evaluated by varying the width of one subsection of the unit cell, i.e. w_2 varied from 0.1 to 0.25 μm in multiples of 0.05 μm and fixing $w_1 = 0.3$ μm. A slight shift in bandgap is observed in the transmission plot due to change in refractive index, which agrees well with (2). When there is a large variation between w_1 and w_2, mode mismatching takes place and a perfect bandgap is observed with near zero transmission. The minor variation between the two widths of the grating structure leads to a reduction in the bandgap and it does not provide near zero transmission in the bandgap. This is clearly observable from Fig. 7.

In order to make a benchmark, the rectangular and sinusoidal Bragg gratings considering the same dimensions are compared, as shown in Fig. 8. For sinusoidal Bragg grating, transmission of >80% is observed in the passband, and at the same time, the transmission in bandgap is near to zero. Contrary to this rectangular Bragg grating exhibits only 60% transmission in the passband, as shown in Fig. 8. The reason behind high transmission in sinusoidal Bragg grating is minimised radiation losses due to smooth variation in structure. However, the bandgap of the sinusoidal grating is somewhat compromised due to less abruptness, but it can be

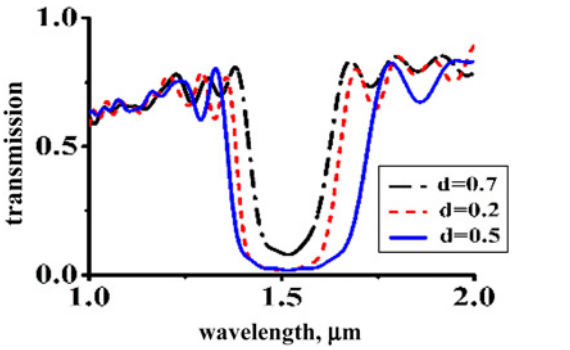

Fig. 4 *Transmission characteristics of Bragg with various duty cycles 0.2, 0.5 and 0.7 for N = 11 cells*

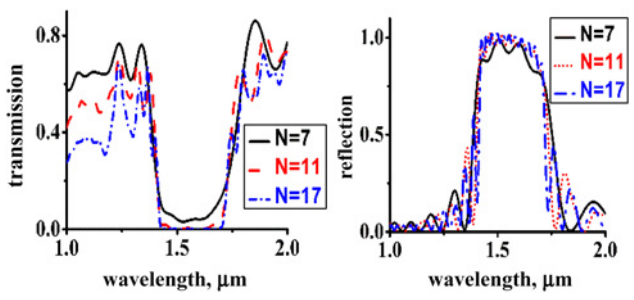

Fig. 5 *Characteristics of sine-shaped Bragg grating for N = 7, 11 and 17 cells*
a Transmission
b Reflection

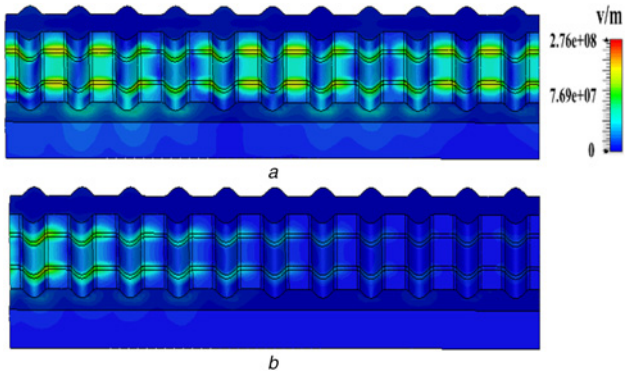

Fig. 6 *3D E-field distribution of HMIM plasmonic sinusoidal Bragg grating for N = 11 at*
a 1.25 μm
b 1.55 μm

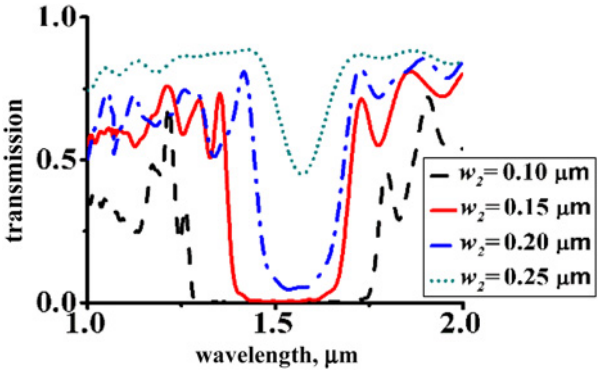

Fig. 7 *Transmission characteristics of sinusoidal Bragg grating with 50% duty cycle, N = 11 cells, $w_1 = 0.3$ μm and w_2 varied from 0.1 to 0.25 μm*

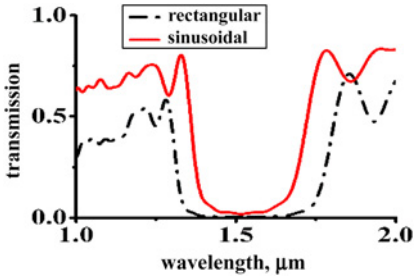

Fig. 8 *Comparison of transmission characteristics of rectangular and sinusoidal Bragg gratings with 50% duty cycle and N = 11 cells*

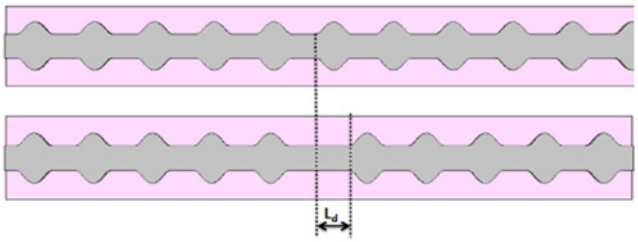

Fig. 9 *Top view of the sine modulated Bragg grating with the addition of defect length L_d*

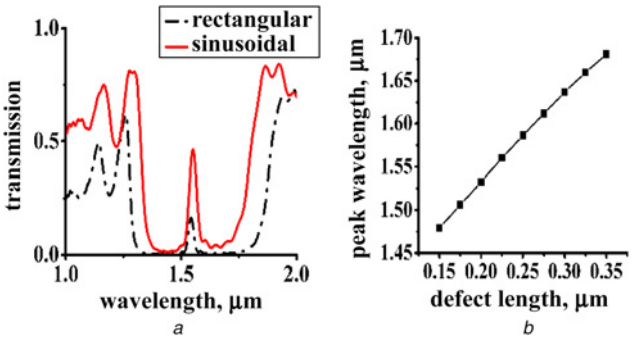

Fig. 10 *Characteristics of resonant cavity*
a Transmission characteristics of defect mode in both rectangular sinusoidal Bragg gratings with $N = 5$ cells on both the sides
b Peak wavelength V/s defect length (L_d) in the case of sinusoidal Bragg grating

increased further by increasing the number of cells. Though sinusoidal Bragg grating provides less bandgap compared to a rectangular one, our results show a wider bandgap of 0.387 μm which is more than that reported in [16, 17].

4. Resonant cavity formation: A resonant cavity is also designed by creating a line defect at the centre unit cell of sinusoidal Bragg grating, as shown in Fig. 9. For that, the length of the centre straight waveguide subsection of a unit cell has been increased, considering $N = 5$ on both the sides. This incremented length is denoted as 'L_d'. Introduced line defect makes a cavity due to which a large portion of incident light is transmitted through the bandgap at the resonance wavelength, which is also called defect mode. The transmission characteristics with defect length $L_d = 0.217$ μm for both sinusoidal and rectangular Bragg gratings are also compared in Fig. 10*a*. The defect length $L_d = 0.217$ μm is chosen by optimising the structure to resonate at 1.55 μm wavelength. Ideally, L_d should be 0.215 μm for achieving resonance at 1.55 μm wavelength, using the following condition: $\lambda_B/4 = L_d + l_2$, but there is a minor shift in resonance, reason being the

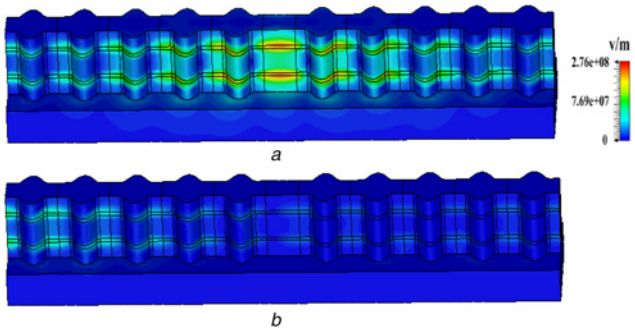

Fig. 11 *3D E-field distribution of HMIM plasmonic sinusoidal Bragg grating for N = 5 on both sides of defect lengths at*
a 1.55 μm
b 1.442 μm

plasmonic effect. A peak transmission of 50% has been observed in the sinusoidal Bragg grating due to the resonance cavity at 1.55 μm wavelength; however rectangular cavity gives very poor transmission of 20% compared to the sinusoidal one. Though the previous reports [16, 17] show a higher peak resonance of nearly 80%, the extinction ratio is not really high as the reflection percentage is very less. Our proposed structure is fruitful in gaining higher reflections as the key objective of Bragg grating is to achieve 100% reflection in the bandgap. Also, a narrow resonance bandwidth of 0.029 μm is achieved due to the microcavity. Peak wavelength with respect to defect length is also plotted in Fig. 10*b* which reveals that the resonance wavelength gets red shifted by increasing the defect length. It proves that the cavity can be tuned according to the required resonance wavelength by simply changing the defect length. The 3D *E*-field view has also been shown at 1.55 μm wavelength, as shown in Fig. 11*a*, which shows that the cavity allows light to pass through defect mode. Contrary to this, Fig. 11*b* shows 3D *E*-field view at 1.442 μm which comes in bandgap region and it does not allow light to reach at the other end. The quality factor is calculated by the ratio of energy stored in the defect at resonance to the energy escaped from the cavity. This is evaluated by using the simple equation $Q = \lambda_B/\Delta\lambda$ where $\Delta\lambda$ denotes full width half maximum bandwidth. Thus the quality factor turned out to be 53 which is higher compared to the one reported in [12].

5. Conclusion: A sinusoidal Bragg grating has been proposed using HMIM waveguide for the first time and deeply analysed. The Bragg resonance condition has been followed and perfect transmission characteristics with a bandgap of 0.387 μm are achieved. Comparison with the previous literature shows that the proposed structure is compact with a track length of 3.784 μm for a minimum number of 11 cells. A microcavity has also been formed by increasing the length of the straight waveguide and its resonance is investigated. A resonance peak of 50% transmission and resonance bandwidth of 0.029 μm is achieved. Also, the quality factor calculated is higher and is about 53. The proposed Bragg grating may find a wide range of applications such as distributed Bragg reflector lasers, add-drop filters, wavelength division multiplexers and so on thus providing a path for achieving large scale integrated photonic devices.

6. References

[1] Ozbay E.: 'Plasmonics: merging photonics and electronics at nanoscale dimensions', *Science*, 2006, **311**, (5758), pp. 189–193
[2] Dai D., He S.: 'A silicon-based hybrid plasmonic waveguide with a metal cap for a nano-scale light confinement', *Opt. Express*, 2009, **17**, pp. 16646–16653

doi: 10.1049/mnl.2018.5107

[3] Oulton R.F., Sorger V.J., Genov D.A., *ET AL.*: 'A hybrid plasmonic waveguide for sub wavelength confinement and long-range propagation', *Nature Photon.*, 2008, **2**, pp. 496–500
[4] Noghani M.T., Samiei M.H.V.: 'Analysis and optimum design of hybrid plasmonic slab waveguides', *Plasmonics*, 2013, **8**, (2), pp. 1155–1168
[5] Chu H.-S., Bai P., Li E.-P., *ET AL.*: 'Hybrid dielectric-loaded plasmonic waveguide-based power splitter and ring resonator: compact size and high optical performance for nano photonic circuits', *Plasmonics*, 2011, **6**, (3), pp. 591–597
[6] Zhu N., Mei T.: 'Analysis of an ultra-compact wavelength filter based on hybrid plasmonic waveguide structure', *Opt. Lett.*, 2012, **37**, pp. 1751–1753
[7] Sharma P., Kumar V.D.: 'Hybrid insulator metal insulator planar plasmonic waveguide-based components', *IEEE Photonics Technol. Lett.*, 2017, **29**, (16), pp. 1360–1363
[8] Sharma P., Kumar V.D.: 'Investigation of multilayer planar hybrid plasmonic waveguide and bends', *Electron. Lett.*, 2016, **52**, (9), pp. 732–734
[9] Sharma P., Kumar V.D.: 'All optical logic gates using hybrid metal insulator metal plasmonic waveguide', *IEEE Photonics Technol. Lett.*, 2018, **30**, (10), pp. 959–962, doi: 10.1109/LPT.2018.2826051
[10] Sharma P., Kumar V.D.: 'Hybrid metal insulator metal plasmonic waveguide and ring resonator'. 2016 21st OptoElectronics and Communications Conf. (OECC) held Jointly with 2016 Int. Conf. Photonics in Switching (PS), Niigata, Japan, 2016, pp. 1–3
[11] Sharma P., Dinesh K.V.: 'Surface Plasmon Bragg grating using hybrid metal insulator metal plasmonic waveguide'. 2017 Progress in Electromagnetics Research Symp. – Fall (PIERS–FALL), Singapore, 2017, pp. 2747–2751
[12] Qu S., Song C., Xia X., *ET AL.*: 'Detuned plasmonic Bragg grating sensor based on a defect metal-insulator-metal waveguide', *Sensors*, 2016, **16**, p. 784
[13] Hosseini A., Nejati H., Massoud Y.: 'Modeling and design methodology for metal-insulator-metal plasmonic Bragg reflectors', *Opt. Express*, 2008, **16**, pp. 1475–1480
[14] Liu J.-Q., Wang L.-L., He M.-D., *ET AL.*: 'A wide band gap plasmonic Bragg reflector', *Opt. Express*, 2008, **16**, pp. 4888–4894
[15] Song C., Xia X., Hu Z-D., *ET AL.*: 'Characteristics of plasmonic Bragg reflectors with graphene-based silicon grating', *Nanoscale Res. Lett.*, 2016, **11**, (1), p. 1
[16] Han Z., Forsberg E., He S.: 'Surface plasmon Bragg gratings formed in metal-insulator-metal waveguides', *IEEE Photonics Technol. Lett.*, 2007, **19**, (2), pp. 91–93
[17] Xu P., Huang Q., Shi Y.: 'Silicon hybrid plasmonic Bragg grating reflectors and high Q-factor micro-cavities', *Opt. Commun.*, 2013, **289**, pp. 81–84
[18] Zhang Z.: 'Silicon based photonic devices: design, fabrication and characterization'. Ph.D. dissertation, Department of Microelectronics and Appl. Phys., Royal Institute of Technology (KTH), Stockholm, Sweden, 2008
[19] Miyazak H.T.: 'Squeezing visible light waves into a 3-nm-thick and 55-nm-long plasmon cavity'. PRL 96, 097401, 2006
[20] Prajapati C.S., Soman R., Rudraswamy S.B., *ET AL.*: 'Single chip gas sensor array for air quality monitoring', *J. Microelectromech. Syst.*, 2017, **26**, (2), pp. 433–439
[21] Johnson P.B., Christy R.W.: 'Optical constants of the noble metals', *Phys. Rev. B*, 1972, **6**, (12), pp. 4370–4379
[22] Zeng R., Zhang Y., Sailing H.E.: 'Energy intensity analysis of modes in hybrid Plasmonic waveguide', *Front. Optoelectron.*, 2012, **5**, (1), pp. 68–72, doi 10.1007/s12200-012-0195-8